



**University of
Zurich**^{UZH}

**Zurich Open Repository and
Archive**

University of Zurich
University Library
Strickhofstrasse 39
CH-8057 Zurich
www.zora.uzh.ch

Year: 2015

Distinguishing Infected From Noninfected Abdominal Fluid Collections After Surgery: An Imaging, Clinical, and Laboratory-Based Scoring System

Gnannt, Ralph ; Fischer, Michael A ; Baechler, Thomas ; Clavien, Pierre-Alain ; Karlo, Christoph ; Seifert, Burkhardt ; Lesurtel, Mickael ; Alkadhi, Hatem

DOI: <https://doi.org/10.1097/RLI.0000000000000090>

Posted at the Zurich Open Repository and Archive, University of Zurich

ZORA URL: <https://doi.org/10.5167/uzh-98694>

Journal Article

Published Version

Originally published at:

Gnannt, Ralph; Fischer, Michael A; Baechler, Thomas; Clavien, Pierre-Alain; Karlo, Christoph; Seifert, Burkhardt; Lesurtel, Mickael; Alkadhi, Hatem (2015). Distinguishing Infected From Noninfected Abdominal Fluid Collections After Surgery: An Imaging, Clinical, and Laboratory-Based Scoring System. *Investigative Radiology*, 50(1):17-23.

DOI: <https://doi.org/10.1097/RLI.0000000000000090>

Distinguishing Infected From Noninfected Abdominal Fluid Collections After Surgery

An Imaging, Clinical, and Laboratory-Based Scoring System

Ralph Gnannt, MD,* Michael A. Fischer, MD,* Thomas Baechler, MD,† Pierre-Alain Clavien, MD, PhD,‡
Christoph Karlo, MD,* Burkhardt Seifert, PhD,‡ Mickael Lesurtel, MD, PhD,†
and Hatem Alkadhi, MD, MPH, EBCR*

Objectives: Mortality from abdominal abscesses ranges from 30% in treated cases up to 80% to 100% in patients with undrained or nonoperated abscesses. Various computed tomographic (CT) imaging features have been suggested to indicate infection of postoperative abdominal fluid collections; however, features are nonspecific and substantial overlap between infected and noninfected collections exists. The purpose of this study was to develop and validate a scoring system on the basis of CT imaging findings as well as laboratory and clinical parameters for distinguishing infected from noninfected abdominal fluid collections after surgery. **Materials and Methods:** The score developmental cohort included 100 consecutive patients (69 men, 31 women; mean age, 58 ± 17 years) who underwent portal-venous phase CT within 24 hours before CT-guided intervention of postoperative abdominal fluid collections. Imaging features included attenuation (Hounsfield unit [HU]), volume, wall enhancement and thickness, fat stranding, as well as entrapped gas of fluid collections. Laboratory and clinical parameters included diabetes, intake of immunosuppressive drugs, body temperature, C-reactive protein, and leukocyte blood cell count. The score was validated in a separate cohort of 30 consecutive patients (17 men, 13 women; mean age, 51 ± 15 years) with postoperative abdominal fluid collections. Microbiologic analysis from fluid samples served as the standard of reference. **Results:** Diabetes, body temperature, C-reactive protein, attenuation of the fluid collection (in HUs), wall enhancement and thickness of the wall, adjacent fat stranding, as well as entrapped gas within the fluid collection were significantly different between infected and noninfected collections ($P < 0.001$). Multiple logistic regression analysis revealed diabetes, C-reactive protein, attenuation of the fluid collection (in HUs), as well as entrapped gas as significant independent predictors of infection ($P < 0.001$) and thus was selected for constructing a scoring system from 0 to 10 (diabetes: 2 points; C-reactive protein, ≥ 100 mg/L: 1 point; attenuation of fluid collection, ≥ 20 HU: 4 points; entrapped gas: 3 points). The model was well calibrated (Hosmer-Lemeshow test, $P = 0.36$). In the validation cohort, scores of 2 or lower had a 90% (95% confidence interval [CI], 56%–100%) negative predictive value, scores of 3 or higher had an 80% (95% CI, 56%–94%) positive predictive value, and scores of 6 or higher a 100% (95% CI, 74%–100%) positive predictive value for diagnosing infected fluid collections. Receiver operating characteristic analysis revealed an area under the curve of 0.96 (95% CI, 0.88–1.00) for the score.

Conclusions: We introduce an accurate scoring system including quantitative radiologic, laboratory, and clinical parameters for distinguishing infected from noninfected fluid collections after abdominal surgery.

Received for publication April 7, 2014; and accepted for publication, after revision, July 17, 2014.

From the *Institute of Diagnostic and Interventional Radiology, and †Department of Surgery, Swiss Hepato-Pancreato-Biliary and Transplantation Center, University Hospital Zurich; and ‡Division of Biostatistics, Institute of Social and Preventive Medicine, University of Zurich, Zurich, Switzerland.

Conflicts of interest and sources of funding: none declared.

Mickael Lesurtel is supported by a professorship grant from the Swiss National Science Foundation (PP00P3_128475).

Reprints: Hatem Alkadhi, MD, MPH, EBCR, Institute of Diagnostic and Interventional Radiology, University Hospital Zurich, Raemistrasse 100, CH-8091 Zurich, Switzerland. E-mail: hatem.alkadhi@usz.ch.

Copyright © 2014 by Lippincott Williams & Wilkins
ISSN: 0020-9996/15/0000-0000

Key Words: computed tomography, fluid collection, abdomen, infection

(*Invest Radiol* 2015;00: 00–00)

Abdominal fluid collections are common after surgery, with a reported prevalence up to 64% in imaging studies.¹ This holds true for various types of abdominal surgery, primarily including gastric and bowel surgery but also procedures such as partial hepatectomy, pancreatectomy, and biliary tract surgery. Depending on their content, fluid collections can be divided into seroma, lymphocele, hematoma, or bilioma.^{2,3} Irrespective of their content, all these fluid collections can get infected, leading to abscess formation. When there is suspicion for abscess formation after surgery, radiologists and surgeons are prompted to consider the underlying etiology of infection such as anastomotic or bile leakage and fistula. In addition, infected abdominal fluid collections often need to be treated, either interventionally or surgically. Thus, the accurate distinction between infected and noninfected abdominal fluid collections after surgery is mandatory to avoid unnecessary treatment.

The differentiation between infected and noninfected fluid collections is important because it influences treatment algorithms toward a more aggressive approach, which, besides an antibiotic regimen, includes percutaneous or surgical drainage.⁴ Mortality from infected abdominal fluid collections ranges from 30% in treated cases up to 80% to 100% in patients with undrained and nonoperated abscesses,⁵ indicating the clinical relevance of an accurate diagnosis in the postoperative setting.

The standard of reference for the diagnosis of infected fluid collections is actually microbiological analysis of fluid samples. Samples are analyzed through microscopic examination and Gram staining. In addition, agar plates are used as media for culturing microorganisms. Infection is considered absent if microscopic and Gram stain as well as cultures are negative.⁶

Although percutaneous drainage of postoperative abdominal fluid collections is usually effective with a treatment success of 90% or higher, a nonnegligible procedure-associated complication rate remains, including septicemia, hemorrhage, and death.^{7–10} Moreover, up to one third of fluid collections cannot be drained completely.^{11,12} Finally, noninfected fluid collections can be an incidental finding after surgery without the need for any treatment, potentially resorbing spontaneously.¹³

Computed tomography (CT) represents the most popular imaging modality for the identification and characterization of postoperative abdominal fluid collections.^{3,14} Fluid attenuation measurements, encapsulation, stranding of the surrounding fat, and the presence of gas within the collection had been proposed as being helpful for differentiating infected from noninfected collections. However, these CT imaging parameters are nonspecific and a substantial overlap between infected and noninfected fluid collections exists.^{3,15,16}

The purpose of this study was to develop and validate a scoring system incorporating CT imaging findings as well as laboratory and

clinical parameters for discriminating infected from noninfected abdominal fluid collections after abdominal surgery.

MATERIALS AND METHODS

Study Population

The retrospective study was approved by the hospital's ethics committee. Written informed consent requirement was waived because no CT was merely performed for the purpose of the study.

Between December 2009 and November 2011, a total of 130 consecutive patients (82 men, 48 women; mean age, 58 ± 15 years) were referred to our radiology department for CT-guided percutaneous drainage of an intraperitoneal and retroperitoneal fluid collection after surgery. Inclusion criteria for study enrollment were previous abdominal surgery (including both laparoscopic and open surgery) and an abdominopelvic CT scan obtained in the portal-venous phase of enhancement within 24 hours before CT-guided intervention. Further inclusion criteria were as follows: microbiologic analysis of the tapped fluid samples, body temperature measurements, and blood sample including white blood cell counts and C-reactive protein within 6 hours before CT-guided intervention.

Exclusion criteria were abdominal fluid collections in solid abdominal organs and those with 1 or more missing laboratory parameters or body temperature measurements ($n = 21$), CT scan without contrast media or CT scan not obtained within 24 hours before CT-guided percutaneous intervention ($n = 7$), as well as missing microbiological results ($n = 2$). Thus, we included a total of 100 patients (69 men, 31 women; mean age 57 ± 15 years) in the first part of the study (Fig. 1; Table 1), which was aimed at the development of the scoring system.

The second part of the study was planned for validating the scoring system. This was performed in a separate cohort of 30 consecutive patients (17 men, 13 women; mean age, 51 ± 15 years) with postoperative abdominal fluid collections referred to our department between December 2011 and June 2012 (Table 1). Similar to the 100 patients in the first study part, all these 30 patients underwent a contrast-enhanced CT acquired during the portal-venous phase within 24 hours before CT-guided percutaneous intervention.

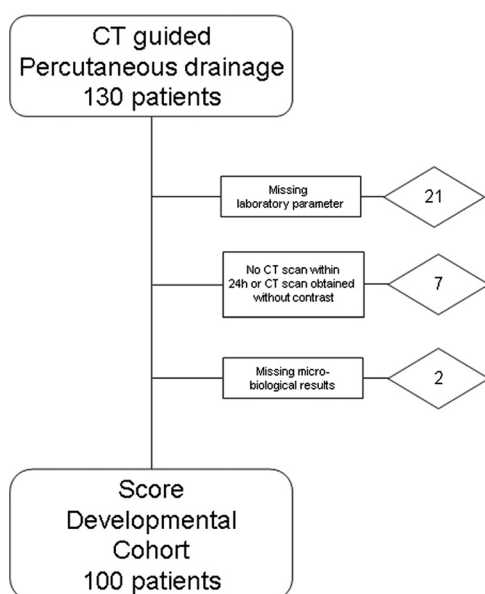


FIGURE 1. Flow chart of the score developmental study cohort.

TABLE 1. Demographic and Clinical Variables of Patients With Postoperative Abdominal Fluid Collections

	Score Development Cohort (n = 100)	Score Validation Cohort (n = 30)
Age, y	57 ± 15 (17–87)	51 ± 15 (21–77)
Sex, male/female	69/31	17/13
Body mass index, kg/m ²	27.2 ± 5.2 (15.1–41.5)	26.9 ± 5.1 (17.1–38.7)
Underlying disease		
Carcinoma	57	16
Infection	24	8
Trauma	6	3
Vascular	7	2
Others	6	1
Surgery before drainage		
Gastrointestinal	34	10
Liver, gallbladder, and spleen	47	14
Peritoneal lavage/exploration	9	3
Urogenital	5	1
Pancreas, kidney, or liver transplantation	5	2

Age and body mass index expressed as mean ± standard deviation (range).

Review of Medical Records and Laboratory Findings

One radiologist (R1, with 2 years of experience in abdominal radiology) reviewed the medical records of all patients in the hospital's electronic medical records system and extracted the following data: age and sex, underlying disease, type of surgery, presence of diabetes (defined according to the American Diabetes Association guidelines¹⁷), time interval between abdominal surgery and CT-guided intervention, actual intake of immunosuppressive drugs (glucocorticoids, cytostatics, antibodies against lymphocytes, drugs acting on immunophilins, interferons, tumor necrosis factor binding proteins), antibiotics, body temperature and blood sample including C-reactive protein, as well as white blood cell counts within 6 hours before percutaneous drainage.

CT Imaging Protocol

All CT studies were performed on a 64-slice CT machine (Definition AS; Siemens Healthcare). In each patient, 90 mL of iopromide (Ultravist 300, 300 mg/mL; Bayer Schering Pharma) were injected at a flow rate of 2.6 mL/s, followed by 40 mL of saline solution at the same flow rate. After a delay of 70 seconds, CT data acquisition was started in the portal-venous phase of enhancement. Automated tube current modulation (CareDose4D; Siemens) was used, with a reference tube current-time product of 150 reference mAs. The other CT parameters were as follows: detector collimation, 32×0.6 mm; slice acquisition, 64×0.6 mm by means of a z-flying focal spot; tube voltage, 120 kV(p); pitch, 1.2; and rotation time, 0.33 seconds.

Images were reconstructed using a medium-smooth soft tissue convolution kernel at a slice thickness of 2 mm and an increment of 1.5 mm.

CT Image Analysis

Computed tomographic data analysis was performed by 2 independent readers (R2, with 5 years and R3, with 9 years of experience in abdominal radiology). Both readers were blinded to the patients' history, laboratory, and microbiological findings as well as to the results of each other. They qualitatively and quantitatively assessed CT images

using the picture archiving and communication system (PACS; IMPAX 5.3, version 6; Agfa, Moertel, Belgium) of the hospital. Multiplanar reformations and arbitrary window width and level settings were allowed. The following parameters were assessed:

- The CT attenuation (in Hounsfield units [HUs]) in a region of interest (average size of approximately 200 mm²) placed within the fluid collection while avoiding partial volume effects from the wall;
- The volume of the encapsulated fluid collection determined by the $ABC/2$ formula, whereas A was the greatest transverse diameter, B was the transverse diameter perpendicular to A , and C was the number of CT slices including the fluid collection multiplied by the effective slice thickness;
- Presence or absence of hypervascular reparative tissue encapsulating the fluid collection, resulting in wall enhancement, defined as a hyperdense rim around the fluid collection;
- Wall thickness (in millimeters) using the electronic caliper tool provided by the PACS software;
- Presence or absence of fat stranding surrounding the fluid collection; and
- Presence or absence of entrapped gas within the collection.

Diagnosis of Infected and Noninfected Fluid Collections

Immediately after CT-guided intervention, at least 5 mL of the drained fluid was sent for microbiological analysis. According to current standards,⁶ fluid was considered infected if leukocytes and bacteria were detected on the Gram stain and/or the culture was positive (bacteria or fungi). Otherwise, the fluid collection was declared as being negative (ie, noninfected).

Statistical Analysis

Continuous variables were expressed as means \pm standard deviations and ranges or as medians and ranges. Categorical variables were expressed as frequencies with percentages.

Interreader agreements for wall enhancement, fat stranding, and gas entrapment were assessed with the Cohen κ statistics ($\kappa > 0.81$, excellent agreement; $\kappa = 0.61$ – 0.80 , good agreement; $\kappa = 0.41$ – 0.60 , moderate agreement; $\kappa = 0.21$ – 0.40 , fair agreement; and $\kappa < 0.20$, poor agreement). Interreader agreements for attenuation, fluid volume, and

wall thickness were assessed with intraclass correlation coefficients (ICCs).

Infected and noninfected fluid collections were compared using the Mann-Whitney U test for the continuous variables and the χ^2 test for the categorical variables. The χ^2 test was also used for testing the relationship between infection as underlying disease necessitating surgery and postoperative infection. Receiver operating characteristic (ROC) analysis with calculation of the area under the curve (AUC) with 95% confidence intervals (CIs) was performed for the parameters showing 2-tailed P values below 0.05 on the univariate analysis.

All these variables were then included into multiple logistic regression analysis. For the multiple regression analysis, the variables were logarithmically transformed (time interval between abdominal surgery and CT-guided intervention and fluid volume), dichotomized at the median (body temperature, C-reactive protein) or visually binned, as appropriate.

Then, the *bestglm* package¹⁸ in R (version 2.15.0) was used for model selection with Bayesian information criterion. Of the top 3 models, we selected the one being most appropriate for daily clinical use.

We then developed a score by rounding the regression coefficients. The ROC analysis reporting the AUC with 95% CI was performed to illustrate the predictive performance of all models. Model calibration was assessed using the Hosmer-Lemeshow test.

Validation of the score was performed in a separate validation set reporting positive (PPV) and negative (NPV) predictive values with 95% CI.

Except for model selection (see above), all analyses were performed using IBM Statistical Package for the Social Sciences Statistics version 20.0 (SPSS Inc, Chicago, IL). Statistical significance was inferred at a P value below 0.05.

RESULTS

CT Image Analysis

Attenuation (ICC, 0.874), volume (ICC, 0.967), and wall thickness (ICC, 0.933) of fluid collections showed a high agreement between the readers. The interreader agreement for wall enhancement ($\kappa = 0.83$; 95% CI, 0.72–0.94), fat stranding ($\kappa = 0.89$; 95% CI,

TABLE 2. Demographics, Laboratory Results, and CT Imaging Findings in the Score Developmental Cohort (n = 100)

	Noninfected Fluid Collections (n = 40)	Infected Fluid Collections (n = 60)	P*
Age, y	58 \pm 17 (17–87)	57 \pm 14 (21–79)	0.53
Sex, male/female	30/10	39/21	0.29
Diabetes	6 (15%)	26 (43%)	0.003
Time interval†, d	86 \pm 26 (1–163)	68 \pm 14 (1–175)	0.74
Immunosuppressive drugs	7 (18%)	8 (13%)	0.57
Antibiotics	24 (60%)	38 (63%)	0.43
Body temperature, °C	37 \pm 0.7 (36–39)	38 \pm 0.7 (36–39)	0.02
C-reactive protein, mg/L	106 \pm 80 (2–276)	155 \pm 103 (11–415)	0.02
Leukocytes, 10 ³ /μL	10.6 \pm 5.9 (4.7–28.4)	12.5 \pm 5.8 (2.5–28.0)	0.06
Attenuation, HU	8 \pm 6 (0.1–26)	17 \pm 9 (2–37)	<0.001
Fluid volume, cm ³	227 \pm 227 (9–1200)	251 \pm 452 (5–1600)	0.1
Wall enhancement	13 (33%)	50 (83%)	<0.001
Wall thickness, mm	1.9 \pm 1.1 (1–5)	2.9 \pm 1.2 (1–7)	<0.001
Fat stranding	11 (28%)	34 (57%)	<0.001
Entrapped gas	3 (8%)	32 (53%)	<0.001

Data are expressed as mean \pm standard deviation (range) or frequencies with percentages.

*Mann-Whitney U Test and Pearson χ^2 test.

†Time interval between surgery and percutaneous drainage.

CT indicates computed tomography; HU, Hounsfield units.

0.73–1.00), and entrapped gas ($\kappa = 0.94$; 95% CI, 0.94–0.98) was excellent. Because of the high agreement between the readers, the results from 1 reader (R2) were used for further analysis.

Univariate Analysis

The results of the univariate analysis are summarized in Table 2. Diabetes, body temperature, C-reactive protein, CT attenuation, wall enhancement, wall thickness, fat stranding, and entrapped gas were significantly different between the infected and noninfected collections (all $P < 0.001$). The highest AUC was found for CT attenuation of the fluid collections (0.80; 95% CI, 0.72–0.89) (Fig. 2). There was no significant relationship between the presence or absence of underlying infection necessitating surgery and postoperative infection ($P = 0.64$).

Model Selection

The use of the *bestglm* command gave rise to different models. From these, we evaluated the top 3 models with the highest AUC. The first one included diabetes, body temperature, CT attenuation, and entrapped gas (AUC, 0.90; 95% CI, 0.84–0.96); the second one included diabetes, CT attenuation, and gas entrapment (AUC, 0.89; 95% CI, 0.82–0.96); and the third model included diabetes, C-reactive protein level, HU value, and gas entrapment (AUC, 0.90; 95% CI, 0.84–0.97).

Because body temperature had a very small standard deviation (0.73) and is influenced by many different factors (eg, fever-reducing drugs, time of measurement throughout the day, type of measurement), we skipped the first model including body temperature having the same AUC as that of model 3. Finally, we chose model 3, which was well calibrated (Hosmer-Lemeshow test, $P = 0.36$) and which discriminated well between the infected and noninfected abdominal fluid collections with an AUC of 0.90 (95% CI, 0.84–0.97).

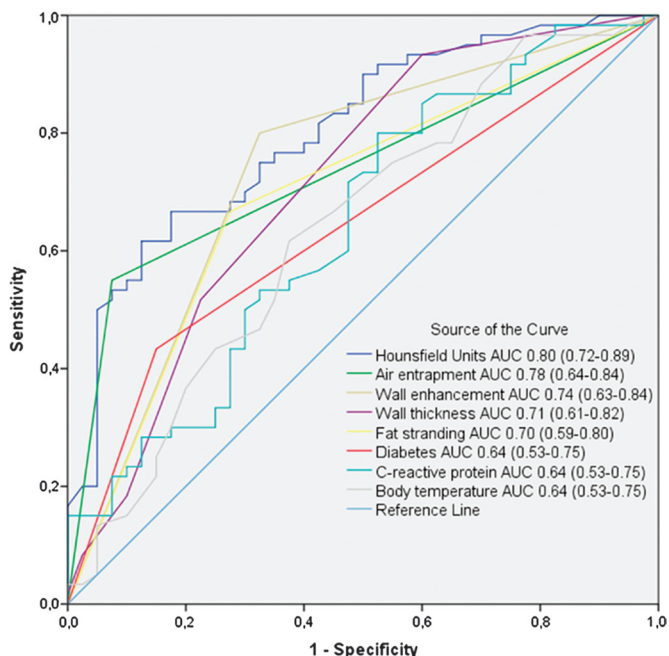


FIGURE 2. Receiver operating characteristic curves for accuracy for radiologic, laboratory, and clinical parameters being significant in the univariate analysis for predicting infected fluid collections in 100 patients. Legend represents AUC with 95% confidence intervals in brackets.

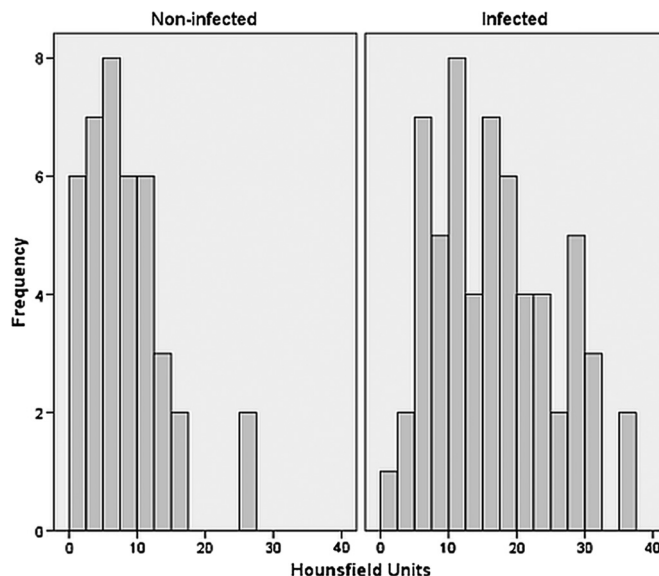


FIGURE 3. Cutoff points for HUs were chosen through visual binning (HU <10 = 0 points; 10 ≤ HU <20 = 2 points; HU ≥20 = 4 points).

Development of the Score

A numerical score was derived from the regression coefficients of the 4 independently significant variables of model 3. The cutoff for the CT attenuation of the fluid was chosen through visual binning (Fig. 3). The cutoff for the C-reactive protein serum level was chosen as the median (113 mg/L). Because the AUC of C-reactive protein was relatively low (0.64), we chose 100 mg/L as a cutoff value for a more easy clinical applicability (reference range of C-reactive protein in our laboratory is <5 mg/L).

The score of each patient was calculated by totaling the scores of each independent variable (Table 3). Using the score in the development cohort, we stratified the patients into 2 groups through visual binning: low (score, ≤2) and high (score, ≥3) probability of having an infected abdominal fluid collection (Fig. 4). In the score developmental cohort, scores of 3 or higher had a PPV of 84% (95% CI, 73%–92%) and a score of 6 or higher had a PPV of 94% (95% CI, 80%–99%). Scores of 2 or lower had an NPV of 91% (95% CI, 75%–98%) for the diagnosis of the infected and noninfected fluid collections, respectively (Table 4).

Validation of the Score

The model validation was performed using a cohort of 30 consecutive patients, in whom complete data to calculate the score were available. In 20 patients with a score of 3 or higher, 4 fluid collections were noninfected (4 false positives). In 10 patients with a score of 2 or lower, 1 collection was infected (1 false negative) (Table 4). Scores of 3 or higher had an 80% (95% CI, 56%–94%) and scores of 6 or higher had a 100% (95% CI, 74–100%) PPV for diagnosing infected fluid collections. The NPV of scores of 2 or lower was 90% (95% CI, 56%–100%). The ROC analysis revealed an AUC of 0.96 (95% CI, 0.88–1.00) for the scoring system. Representative image examples of the patients with infected and noninfected fluid collections are provided in Figures 5 and 6.

DISCUSSION

Percutaneous catheter drainage is the treatment of choice for potentially infected abdominal fluid collections, if there is no evident underlying etiology requiring immediate surgery (such as anastomotic

TABLE 3. Final Model Using Parameters Found to be Independently Predictive of Infected Abdominal Fluid Collections Based on Multiple Regression Analysis

	β (Regression Coefficient)	Points
Diabetes		
No	0	0
Yes	1.7	2
C-reactive protein, mg/L		
<100	0	0
≥ 100	0.9	1
Gas entrapment		
No	0	0
Yes	2.7	3
CT attenuation, HU		
<10	0	0
$10 \leq \text{HU} < 20$	1.7	2
≥ 20	3.4	4
Minimum total score		0
Maximum total score		10

HU indicates Hounsfield units.

leakage).^{19,20} In our cohort with a total of 130 patients, however, 40% of drained fluid collections were not infected, which is comparable with the number reported in previous studies.^{11,15,21} Thus, an intervention aiming at draining infection would not have been necessary in these patients. On the basis of this clinical experience, we developed and validated a score for a better distinction between infected and noninfected abdominal fluid collections after surgery using quantitative information from imaging, clinical, and laboratory data.

For the development of the score, we analyzed 5 clinical/laboratory parameters: presence of diabetes, intake of immunosuppressive drugs,

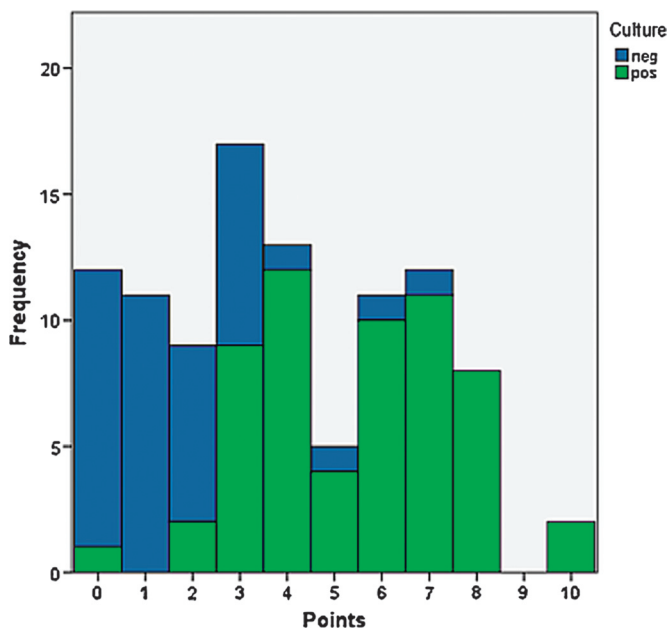


FIGURE 4. Histogram of the score distribution in the 100 patients of the score developmental cohort. On the basis of this graph, we stratified patients into 2 groups: scores 0 to 2, low probability; scores 3 to 10, high probability of having an infected fluid collection.

TABLE 4. Performance of the Scoring System in the Score Developmental and in the Score Validation Cohorts

	Noninfected Fluid Collections	Infected Fluid Collections
Score developmental cohort	(n = 40)	(n = 60)
Low probability (score, 0–2)	29 (73%)	3 (5%)
High probability (3–10)	11 (27%)	57 (95%)
Score validation cohort	(n = 13)	(n = 17)
Low probability (score, 0–2)	9 (69%)	1 (6%)
High probability (3–10)	4 (31%)	16 (94%)

body temperature, C-reactive protein serum level, and leukocyte blood cell counts. Previous studies demonstrated a high correlation between diabetes and postoperative abdominal abscesses and infections after surgery.^{22,23} This is in line with our results indicating that the presence of diabetes is a risk factor for infection of an abdominal fluid collection after surgery.

Patients receiving immunosuppressive medication such as glucocorticoids, cytostatics, antibodies against lymphocytes, drugs acting on immunophilins, interferons, and tumor necrosis factor binding proteins can develop severe lymphopenia, which is deemed to be a risk factor for infections.²⁴ Our results, however, showed no relationship between the intake of immunosuppressive drugs and postoperative infected fluid collections, similar to a recent study by Bafford et al²⁵ in patients with Crohn disease in whom intake of immunosuppressive medication was not associated with an increase in postoperative infections.

In our score developmental cohort, body temperature showed good predictive capabilities regarding the differentiation between infected and noninfected fluid collections. However, because of its small standard deviation (0.73); many potential measurement biases such as intake of fever-reducing drugs, circadian undulation of body temperature, type and location of measurement; and its unspecific character being not necessarily related to infection,²⁶ we did not include body temperature in our scoring system.



FIGURE 5. Contrast-enhanced abdominal CT scan of a 43-year-old man 9 days after surgical treatment of duodenal perforation showing an encapsulated fluid collection with gas entrapment adjacent to the left liver lobe (a). The corresponding score in this patient was 8 (diabetes present; C-reactive protein, 254 mg/L; gas entrapment present; CT attenuation of the fluid collection, 16 HU), indicating a high probability of infection. Percutaneous puncture and drainage were performed, and microbiologic testing revealed infection of the fluid collection with *Escherichia coli*.



FIGURE 6. Contrast-enhanced abdominal CT scan of a 52-year-old woman 12 days after atypical left liver resection for a hepatocellular carcinoma. A fluid collection without gas is depicted in the area of resection. The score in this patient was 2 (no diabetes; C-reactive protein, 74 mg/L; no gas entrapment; CT attenuation of the fluid collection, 12 HU), indicating a low probability of infection. Percutaneous puncture and drainage were performed, and microbiologic testing revealed a sterile fluid collection.

C-reactive protein and leukocyte blood cell counts are commonly used in clinical routine for determining the presence or absence of infection. The specificity of C-reactive protein is limited in patients after surgery because it might be increased postoperatively also in the absence of infection. In our study group, C-reactive protein was significantly higher in infected as compared with noninfected fluid collections and was an independent predictor of infection based on the multiple regression analysis. Thus, we included this laboratory parameter with a cutoff value of 100 mg/L, for a more easy clinical applicability, into the scoring system.

We included into our analysis various CT imaging features such as wall enhancement and wall thickness, entrapped gas, surrounding fat stranding, and attenuation of the fluid collection. The presence and enhancement of the wall surrounding fluid collections are related to fibrin, which represents a defense mechanism for localizing and limiting peritoneal infections.²⁷ In our population, wall thickness and presence or absence of wall enhancement distinguished well infected from noninfected fluid collections. However, both parameters were not included in the top 3 models from the multiple logistic regression analysis and thus were not implemented in the scoring system.

The presence of gas within a fluid collection has been repetitively shown to be a good predictor for infected fluid collections.^{21,28} This was also confirmed in our study both in the univariate and multiple regression analyses. Thus, we included this imaging feature into the score.

Fat stranding is an unspecific sign of inflammation occurring also in other conditions such as ischemia, bowel perforation, and, after surgery, in the absence of infection.²⁹ This is also reflected in our study population in which 28% of sterile fluid collections showed adjacent fat stranding. Whereas fat stranding showed in the univariate analysis a significant difference between infected and noninfected fluid collections, the parameter was not significant in the multiple regression analysis. Thus, fat stranding was not implemented as an imaging feature into the final score.

The underlying hypothesis of measuring attenuation of fluid collections is that debris in an infected fluid collection leads to higher CT attenuation.³ Previous studies were contradictory regarding the value of attenuation measurements. Whereas earlier studies reported near-water attenuation of infected collections,^{15,28} a recent study

showed attenuation values higher than 20 HU when infection was present.²¹ In our patients, attenuation measurements allowed discriminating well infected from noninfected collections, with only 2 patients with noninfected collections having attenuation values higher than 20 HU. Hemorrhage into the fluid cavity might be a reason for higher attenuation values of these noninfected collections.

Only few prior studies have combined more than 1 imaging feature for improving the accuracy of diagnosing infected collections. Jaques et al¹⁶ reviewed CT examinations of 71 patients, recording the features of abscess wall, septation, gas/fluid level, presence of a sharp margin, and presence of gas bubbles. In their study, 69% of patients had 1 or more and only 6% had 3 of the features mentioned previously. Allen et al²¹ showed in their study that gas entrapment and fluid attenuation were significant predictors of infection. However, their good sensitivity (83%) was associated with a low specificity (39%).

We used a different approach by developing a scoring system with inclusion of clinical and laboratory parameters as well and by performing a multiple logistic regression analysis. This approach results in a different weighting of the various imaging, clinical, and laboratory findings based on their individual regression coefficients and, hence, in different points in the scoring system for each parameter. By doing so, we could demonstrate in our validation cohort a high accuracy of the score (AUC of 0.96), a PPV of 80% for scores of 3 or higher, a PPV of 100% for scores of 6 or higher, and an NPV of 90% for scores of 2 or lower. Considering both development and validation cohorts, 42 of the 130 patients had scores of 2 or lower, indicating low probability of infection. This means that 42 interventions would have been avoided when relying on the score. Of these 42 fluid collections, 38 turned out to be sterile. Forty-four of the patients had scores of 6 or higher, indicating high probability of infection. Among them, 42 patients had truly infected collections.

From the patients with a positive culture, 2 had positive imaging findings in regard to gas entrapment and HU greater than 20 but with negative clinical and laboratory parameters (no diabetes and C-reactive protein, <100 mg/L). Two patients had negative imaging findings (according to our scoring system) but positive clinical and laboratory parameters. Vice versa, in the patients with negative culture, there was 1 patient with negative imaging findings and positive clinical and laboratory parameters as well as 1 patient with positive imaging findings and negative clinical and laboratory parameters.

We have to acknowledge the following study limitations. First, fluid collections may be symptomatic without being infected and are therefore still requiring intervention. Certainly, our score does not apply for such situations. Second, this study suffers from inherent limitations of retrospective study designs. Future studies should evaluate the value of integrating the score into daily clinical routine in a prospective cohort of patients. Third, CT examinations in this study were performed with a fixed tube potential of 120 kV(p), but the use of recently introduced automated attenuation-based tube voltage selection algorithms³⁰ would result in different attenuation measurements and, consequently, in different thresholds for the scoring system. Finally, we used single-energy but not dual-energy CT, the latter known to improve tissue characterization in various body regions and applications.^{31,32}

In conclusion, we introduce an objective, easy-to-use scoring system including quantitative radiologic, laboratory, and clinical information that helps discriminating infected from noninfected postoperative fluid collections. This score might be helpful to decide for the appropriate treatment strategy in patients with postoperative abdominal fluid collections.

REFERENCES

1. Krumenacker JH, Panicek DM, Ginsberg MS, et al. CT in searching for abscess after abdominal or pelvic surgery in patients with neoplasia: do abdomen and pelvis both need to be scanned? *J Comput Assist Tomogr.* 1997;21:652-655.

2. Brook I. Microbiology and management of abdominal infections. *Dig Dis Sci*. 2008;53:2585–2591.
3. Sirinek KR. Diagnosis and treatment of intra-abdominal abscesses. *Surg Infect (Larchmt)*. 2000;1:31–38.
4. Zimmerman LH, Tyburski JG, Glowinski J, et al. Impact of evaluating antibiotic concentrations in abdominal abscesses percutaneously drained. *Am J Surg*. 2011;201:348–352.
5. Ariel IM, Kazarian KK. Classification, diagnosis and treatment of subphrenic abscesses. *Rev Surg*. 1971;28:1–21.
6. Winn W. *Koneman's Color Atlas and Textbook of Diagnostic Microbiology*. Lippincott Williams & Wilkins. 1997:2–110.
7. vanSonnenberg E, Wittich GR, Goodacre BW, et al. Percutaneous abscess drainage: update. *World J Surg*. 2001;25:362–369.
8. Gee MS, Kim JY, Gervais DA, et al. Management of abdominal and pelvic abscesses that persist despite satisfactory percutaneous drainage catheter placement. *AJR Am J Roentgenol*. 2010;194:815–820.
9. Gervais DA, Ho CH, O'Neill MJ, et al. Recurrent abdominal and pelvic abscesses: incidence, results of repeated percutaneous drainage, and underlying causes in 956 drainages. *AJR Am J Roentgenol*. 2004;182:463–466.
10. Maher MM, Gervais DA, Kalra MK, et al. The inaccessible or undrainable abscess: how to drain it. *Radiographics*. 2004;24:717–735.
11. vanSonnenberg E, Mueller PR, Ferrucci JT Jr. Percutaneous drainage of 250 abdominal abscesses and fluid collections. Part I: results, failures, and complications. *Radiology*. 1984;151:337–341.
12. Kim YJ, Han JK, Lee JM, et al. Percutaneous drainage of postoperative abdominal abscess with limited accessibility: preexisting surgical drains as alternative access route. *Radiology*. 2006;239:591–598.
13. Sawhney R, D'Agostino HB, Zinck S, et al. Treatment of postoperative lymphoceles with percutaneous drainage and alcohol sclerotherapy. *J Vasc Interv Radiol*. 1996;7:241–245.
14. Halber MD, Daffner RH, Morgan CL, et al. Intraabdominal abscess: current concepts in radiologic evaluation. *AJR Am J Roentgenol*. 1979;133:9–13.
15. Haaga JR, Alfidi RJ, Havrilla TR, et al. CT detection and aspiration of abdominal abscesses. *AJR Am J Roentgenol*. 1977;128:465–474.
16. Jaques P, Mauro M, Safrit H, et al. CT features of intraabdominal abscesses: prediction of successful percutaneous drainage. *AJR Am J Roentgenol*. 1986;146:1041–1045.
17. American Diabetes Association. Standards of Medical Care in Diabetes – 2013. *Diabetes Care*. 2013;36(suppl 1):11–66.
18. McLeod AI, Changjiang Xu. bestglm: R package version 0.33. Available at <http://cran.r-project.org/web/packages/bestglm/bestglm.pdf>. Accessed March 28, 2013.
19. Gerzof SG, Robbins AH, Johnson WC, et al. Percutaneous catheter drainage of abdominal abscesses: a five-year experience. *N Engl J Med*. 1981;305:653–657.
20. Johnson WC, Gerzof SG, Robbins AH, et al. Treatment of abdominal abscesses: comparative evaluation of operative drainage versus percutaneous catheter drainage guided by computed tomography or ultrasound. *Ann Surg*. 1981;194:510–520.
21. Allen BC, Barnhart H, Bashir M, et al. Diagnostic accuracy of intra-abdominal fluid collection characterization in the era of multidetector computed tomography. *Am Surg*. 2012;78:185–189.
22. Ming PC, Yan TY, Tat LH. Risk factors of postoperative infections in adults with complicated appendicitis. *Surg Laparosc Endosc Percutan Tech*. 2009;19:244–248.
23. Trinh JV, Chen LF, Sexton DJ, et al. Risk factors for gram-negative bacterial surgical site infection: do allergies to antibiotics increase risk? *Infect Control Hosp Epidemiol*. 2009;30:440–446.
24. Gluck T, Kiefmann B, Grohmann M, et al. Immune status and risk for infection in patients receiving chronic immunosuppressive therapy. *J Rheumatol*. 2005;32:1473–1480.
25. Bafford AC, Powers S, Ha C, et al. Immunosuppressive therapy does not increase operative morbidity in patients with Crohn's disease. *J Clin Gastroenterol*. 2013;47:491–495.
26. Circiumaru B, Baldock G, Cohen J. A prospective study of fever in the intensive care unit. *Intensive Care Med*. 1999;25:668–673.
27. Peritonitis and other intraabdominal infections. In: Howard RJ, Simmons RL, eds. *Surgical Infectious Diseases*. Norwalk, CT: Appleton & Lange; 1988:605.
28. Ferrucci JT Jr, vanSonnenberg E. Intra-abdominal abscess. Radiological diagnosis and treatment. *JAMA*. 1981;246:2728–2733.
29. Pereira JM, Sirlin CB, Pinto PS, et al. Disproportionate fat stranding: a helpful CT sign in patients with acute abdominal pain. *Radiographics*. 2004;24:703–715.
30. Winklehner A, Goetti R, Baumüller S, et al. Automated attenuation-based tube potential selection for thoracoabdominal computed tomography angiography: improved dose effectiveness. *Invest Radiol*. 2011;46:767–773.
31. Artz NS, Hines CD, Brunner ST, et al. Quantification of hepatic steatosis with dual-energy computed tomography: comparison with tissue reference standards and quantitative magnetic resonance imaging in the ob/ob mouse. *Invest Radiol*. 2012;47:603–610.
32. Morsbach F, Wurnig MC, Müller D, et al. Feasibility of single-source dual-energy computed tomography for urinary stone characterization and value of iterative reconstructions. *Invest Radiol*. 2014;49:125–130.